Grazing incidence EXAFS

Outline

optional → Excursion to BL6-2 and TXM-XANES

- Walk through history
- Surface EXAFS
- Grazing incidence and the total reflection of X-rays
  - the penetration depth
  - anomalous dispersion
  - the x-ray standing wave field
  - self-absorption effects
- Example:

  Characterization of ultra shallow junctions by GI-XAS

XAS

XAFS

μXAS

SEXAFS

EXAFS

X-ray Absorption

ReflEXAFS

XANES

NEXAFS

SCOPUS search for publications, June 24th 2011:

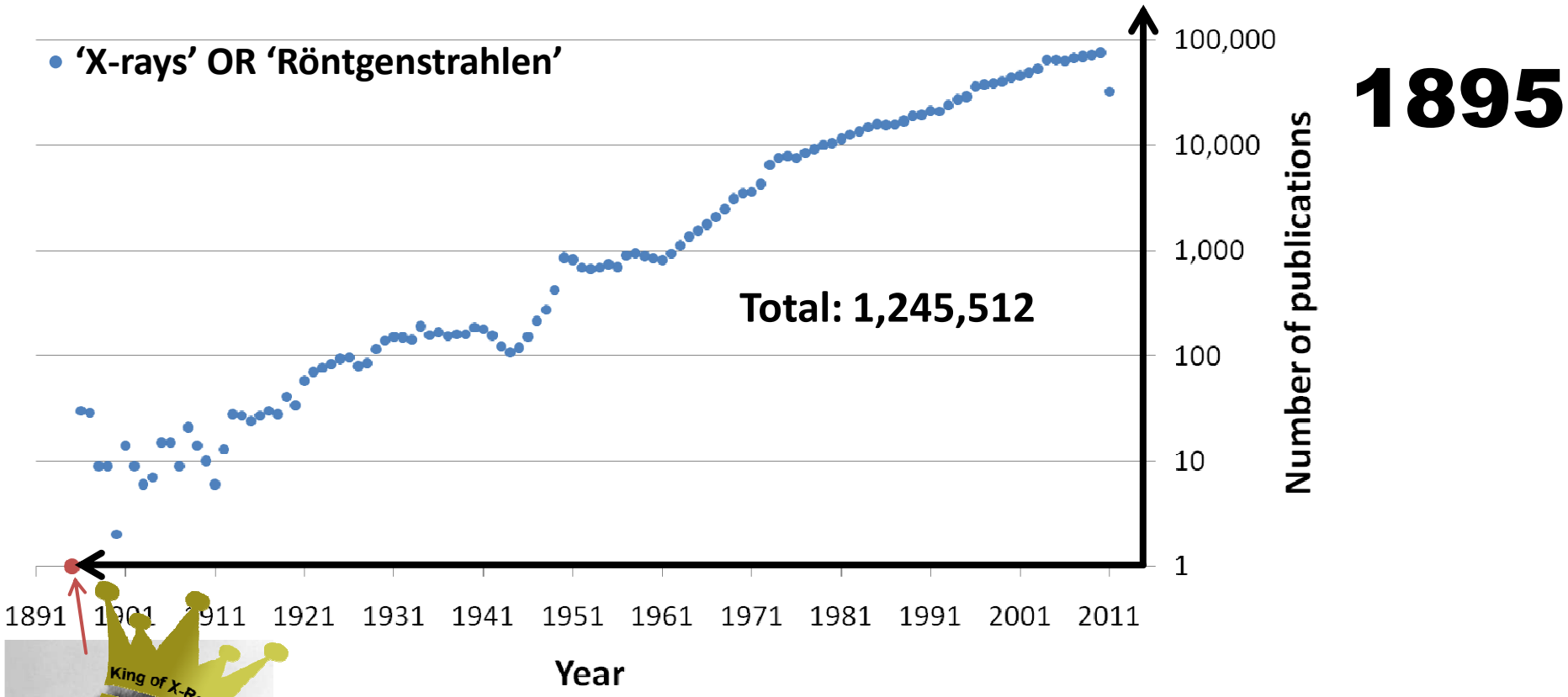

1895

'Der Kürze halber möchte ich den Ausdruck "Strahlen" und zwar zur Unterscheidung von anderen den Namen "X-Strahlen" gebrauchen.'

To shorten I shall use the designation "rays", and to differentiate it from the other ones, the naming **"X-rays"**.

RÖNTGEN W. C., Über eine neue Art von Strahlen, Sitzungsberichte Phys. Mediz. Gesellschaft zu Würzburg 137 (1895) 132-141

SCOPUS search for publications, June 24th 2011:

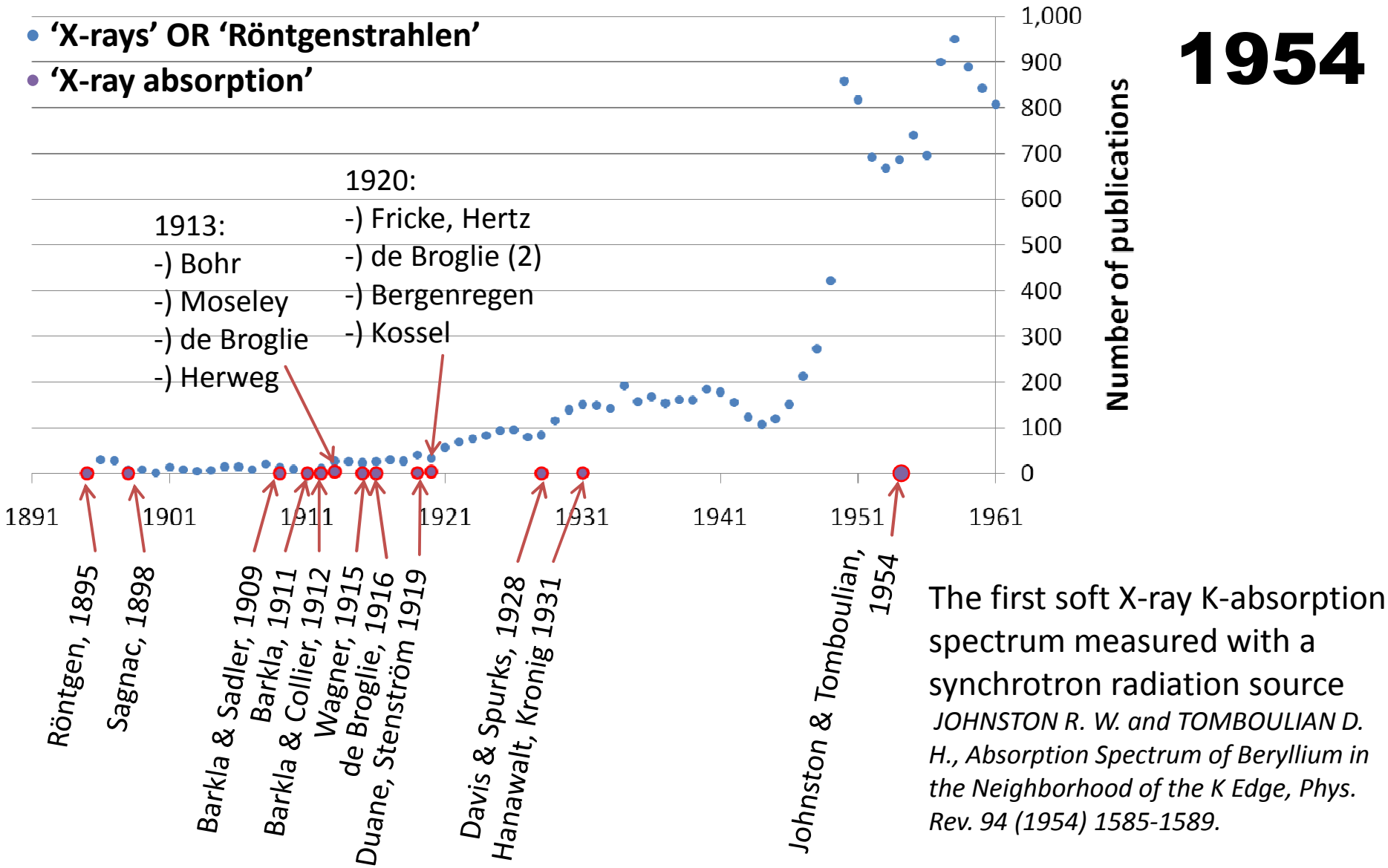

1954

The first soft X-ray K-absorption spectrum measured with a synchrotron radiation source

JOHNSTON R. W. and TOMBOULIAN D. H., Absorption Spectrum of Beryllium in the Neighborhood of the K Edge, Phys. Rev. 94 (1954) 1585-1589.

SCOPUS search for publications, June 24th 2011:

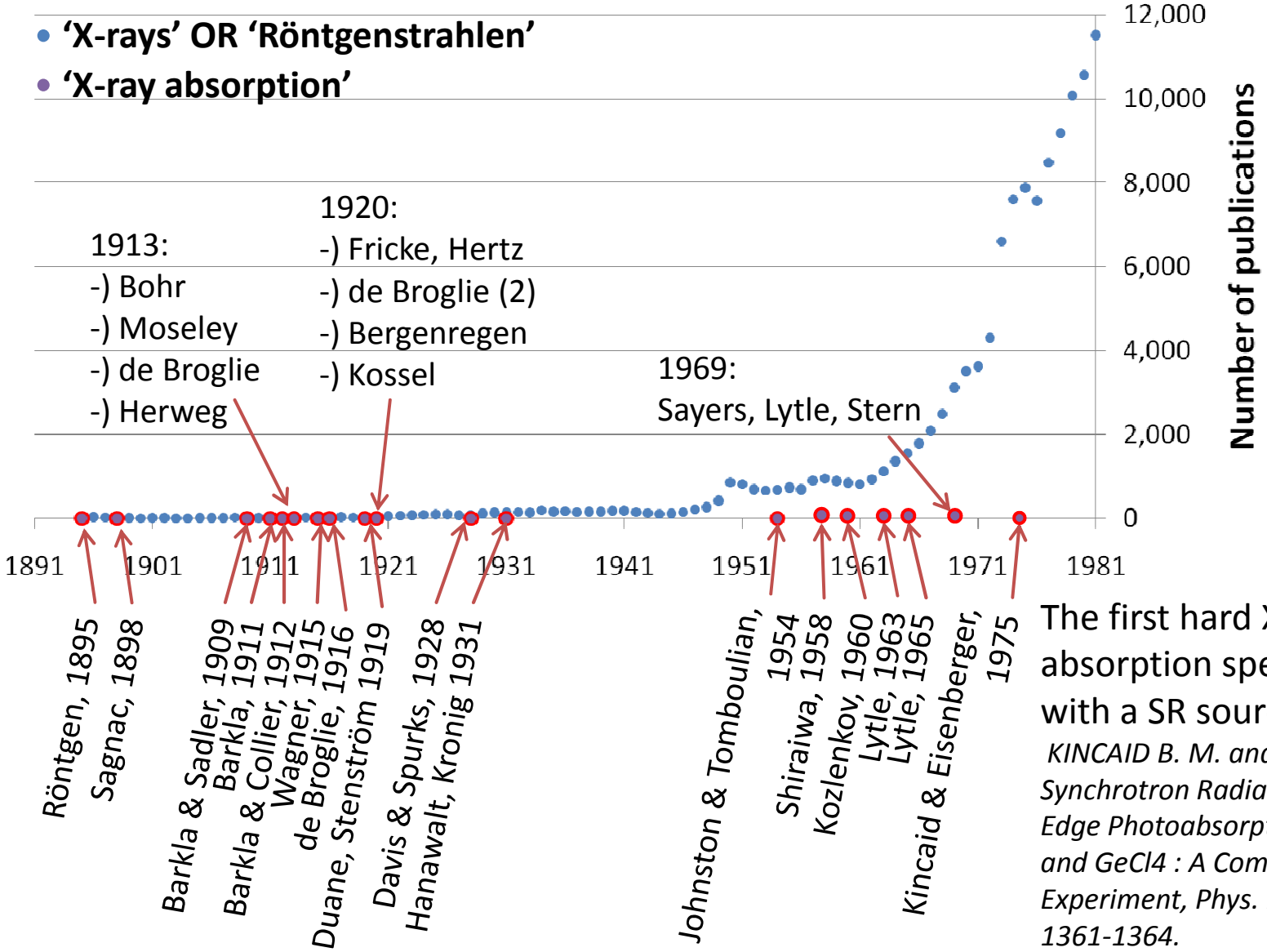

1975

The first hard X-ray K-absorption spectrum measured with a SR source

KINCAID B. M. and EISENBERGER P., Synchrotron Radiation Studies of the K-Edge Photoabsorption Spectra of Kr, Br2, and GeCl4 : A Comparison of Theory and Experiment, Phys. Rev. Lett. 34 (1975) 1361-1364.

SCOPUS search for publications, June 24th 2011:

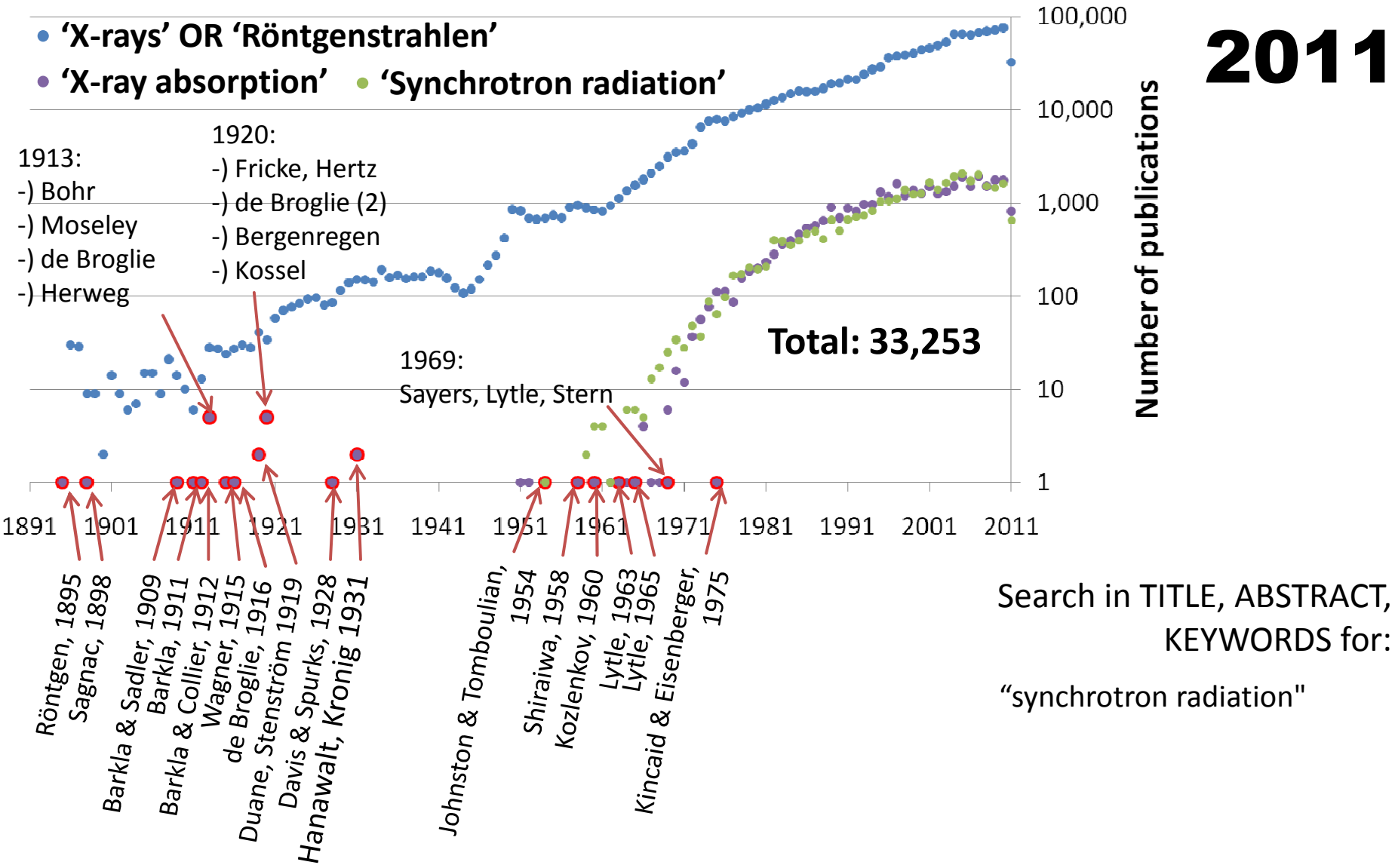

2011

Search in TITLE, ABSTRACT, KEYWORDS for:

"synchrotron radiation"

30 June 1978, Volume 200, Number 4349 SCIENCE

EXAFS: New Horizons in Structure Determinations

P. Eisenberger and B. M. Kincaid

As early as the 1930's, it had been observed that the absorption cross section in the x-ray regime had a complex structure as a function of energy extending as far as 1000 electron volts above an absorption threshold (*I*). These measure- perimental advances the meas were difficult and time-consu cause of the low power of source. This limited the appli the technique to highly concent tems and also inhibited the s

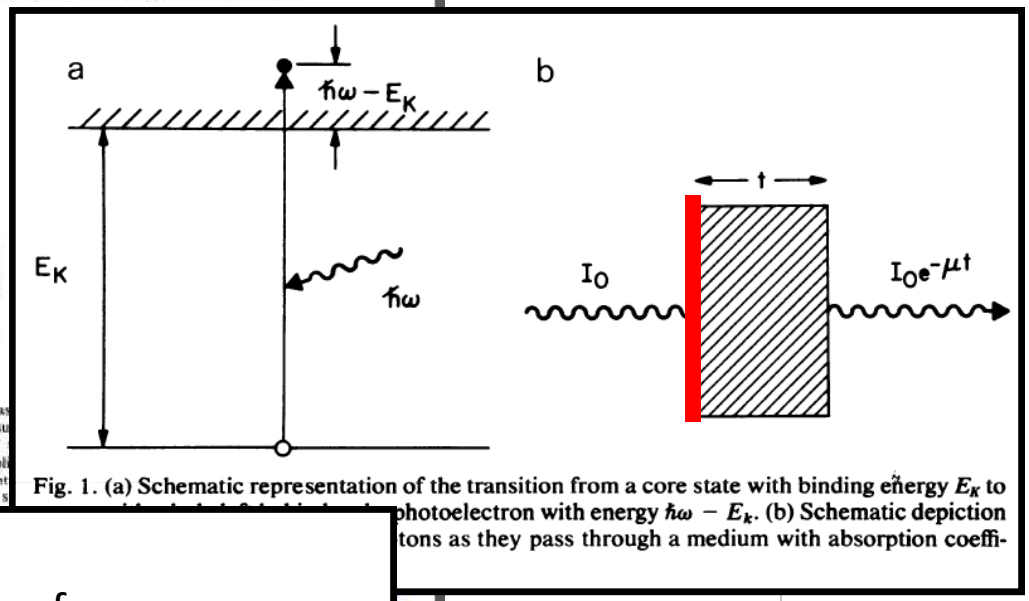

Fig. 1. (a) Schematic representation of the transition from a core state with binding energy E_K to photoelectron with energy $\hbar\omega - E_k$. (b) Schematic depiction tons as they pass through a medium with absorption coeffi-

"For dilute impurities
or adsorbed species on a surface,
the ability to isolate the absorption
signal of the atom of interest by using
fluorescence or Auger detection
greatly enhances the sensitivity of the
technique to the structure of interest."
[…]
"As in fluorescence work, each atom is
characterized by specific Auger energies."

1978

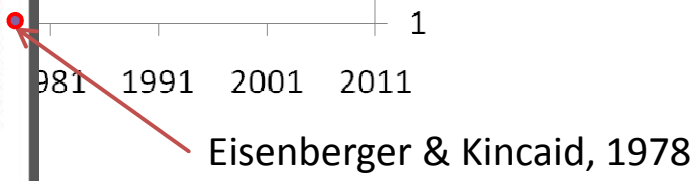

Eisenberger & Kincaid, 1978

1976
1977
1978

Figure a: [Stöhr 96]
Schematic diagram of a photon absorption process resulting in a photoelectron and a core hole. The hole is filled
-) radiatively -> emission of fluorescent photon
-) non-radiatively -> emission of an Auger electron

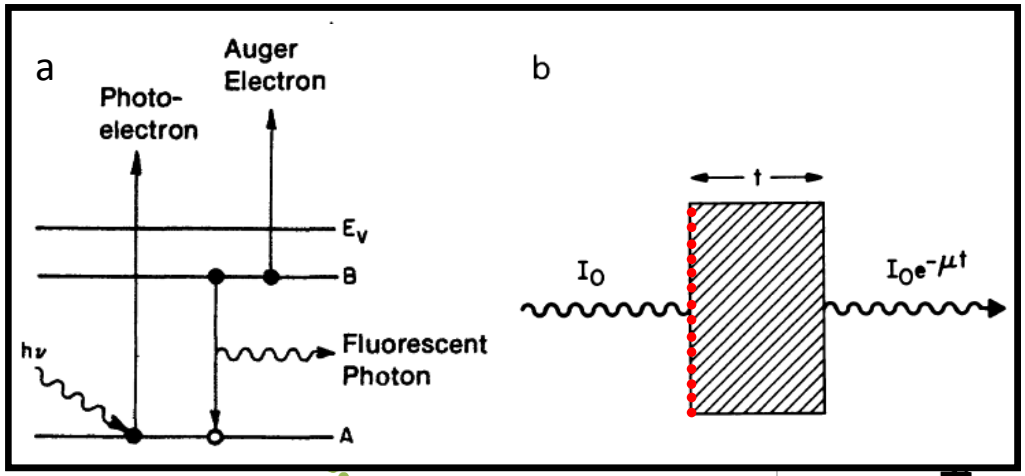

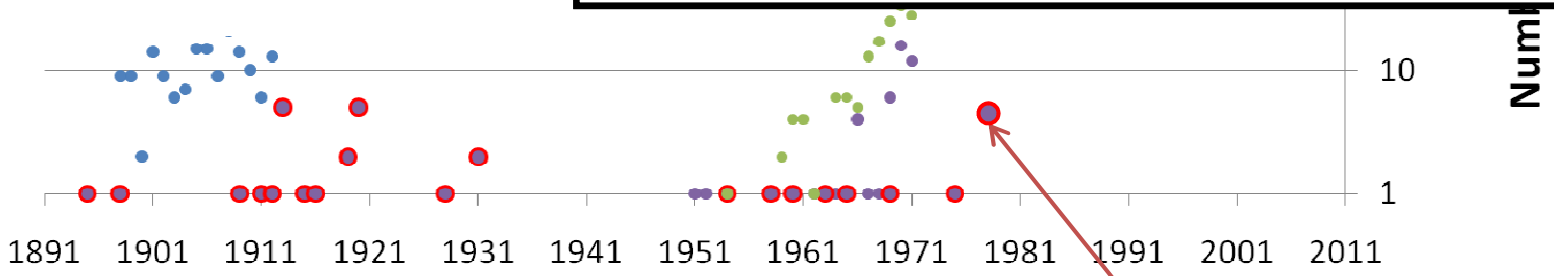

Eisenberger & Kincaid, 1978
Lee, 1976
Citrin, 1977 & 1978 → **"SEXAFS"**
Stöhr, 1978

-) P.A. Lee, Phys. Rev. B13 (1976) 5261.
-) P.H. Citrin, Bull. Am. Phys. Soc. 22 (1977) 359.
-) P.H. Citrin, P. Eisenberger, R.C. Hewitt, J. Vac. Sci. Technol. 15 (1978) 449.
-) J. Stöhr, D. Denley, P. Perfetti, Phys. Rev. B, 18 8 (1978) 4132-4135

Figure a: [Stöhr 96]
Schematic diagram of a photon absorption process resulting in a photoelectron and a core hole. The hole is filled
-) radiatively -> emission of fluorescent photon
-) non-radiatively -> emission of an Auger electron

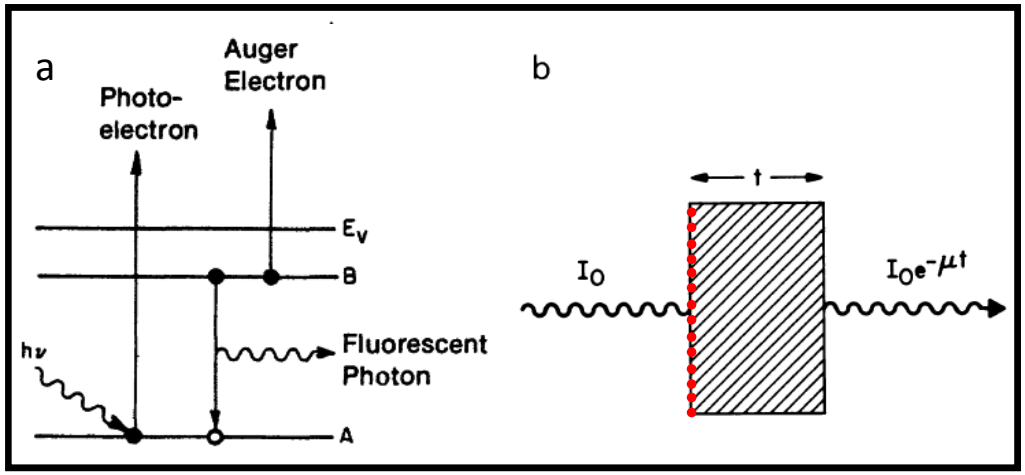

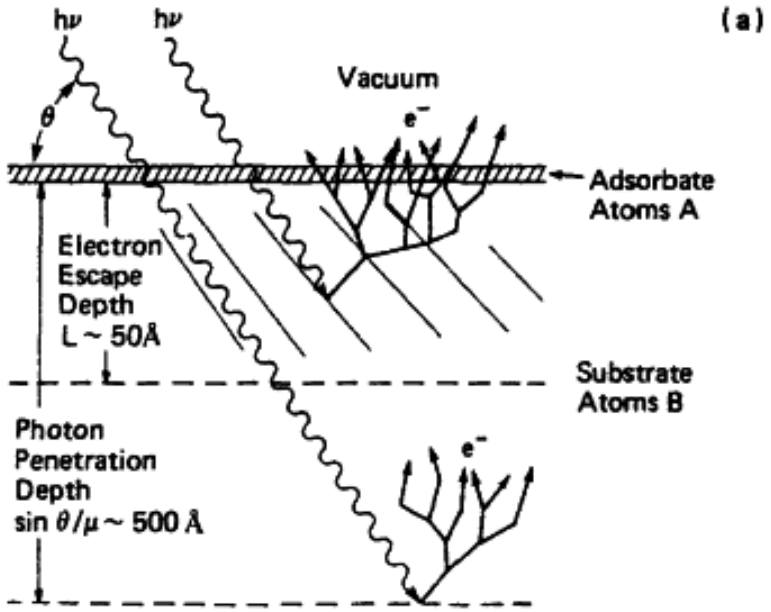

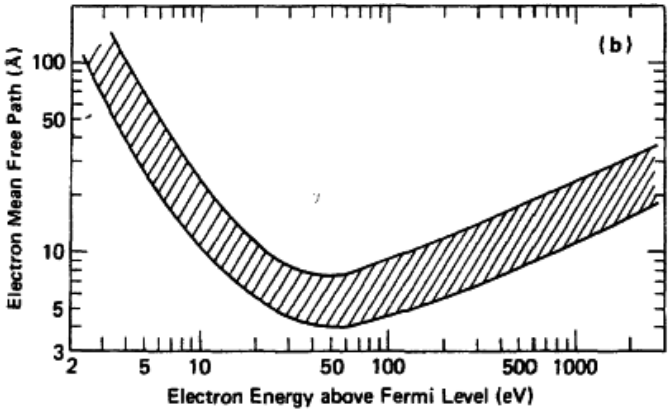

[Stöhr 96]

Fig. 5.6. (a) Photoabsorption and electron production in a sample consisting of substrate atoms B and an adsorbate layer A. Only electrons created within a depth L from the surface contribute to the measured electron yield signal. Electrons originating from layer A constitute the NEXAFS signal; those from layer B give rise to unwanted background. (b) Electron mean free path in solids as a function of the electron kinetic energy above the Fermi level. The shaded area represents the distribution typically found for different materials [5.26, 27]

Figure a: [Stöhr 96]
Schematic diagram of a photon absorption process resulting in a photoelectron and a core hole. The hole is filled
-) radiatively -> emission of fluorescent photon
-) non-radiatively -> emission of an Auger electron

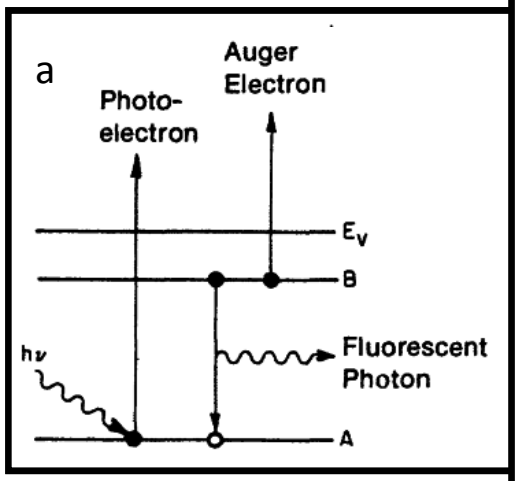

The fractions of the radiative and non-radiative decay rates are called Auger yield ω_a and fluorescence yield ω_f and satisfy the sum rule: $\omega_a + \omega_f = 1$
Auger yield and fluorescence yield are a function of atomic number Z

Can we make it surface sensitive?

TEY	PY	A	FY
Simplicity	Surface sensitivity	Surface sensitivity	Signal/background
Low cost			Sensitivity for high Z
Signal/noise			Two-photon process
Non-UHV			
Absolute sensitivity	Low signal/noise		Diffraction peaks for high Z cost
Signal/background	Interference with photoemission peaks and substrate diffraction peaks		Low counting rate

Table 1: [Lagarde 01]
Qualities (top) and pitfalls (bottom) of the different detection methods

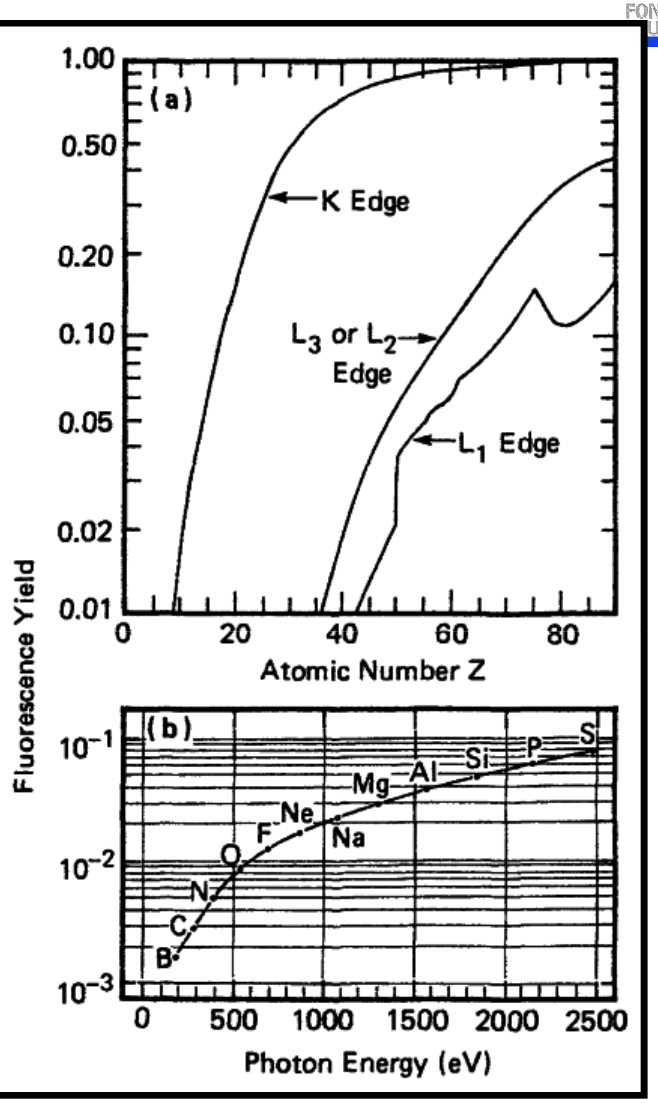

Figure above: [Stöhr 96]
a) Fluorescence yields as a function of atomic number Z
b) Fluorescence yields for the K-shell excitation of low Z atoms

J. Phys. C: Solid St. Phys., 13 (1980) L249–53. Printed in Great Britain

LETTER TO THE EDITOR

Yes, we can (in theory, 1980)…

EXAFS and surface EXAFS from measurements of x-ray reflectivity†

R Fox and S J Gurman

and experiment (1981):

The extended x-ray absorption fine structure in the reflectivity at the K edge of Cu

"ReflEXAFS"

G Martens and P Rabe

Institut für Experimentalphysik, Universität Kiel, D-2300 Kiel 1, West Germany

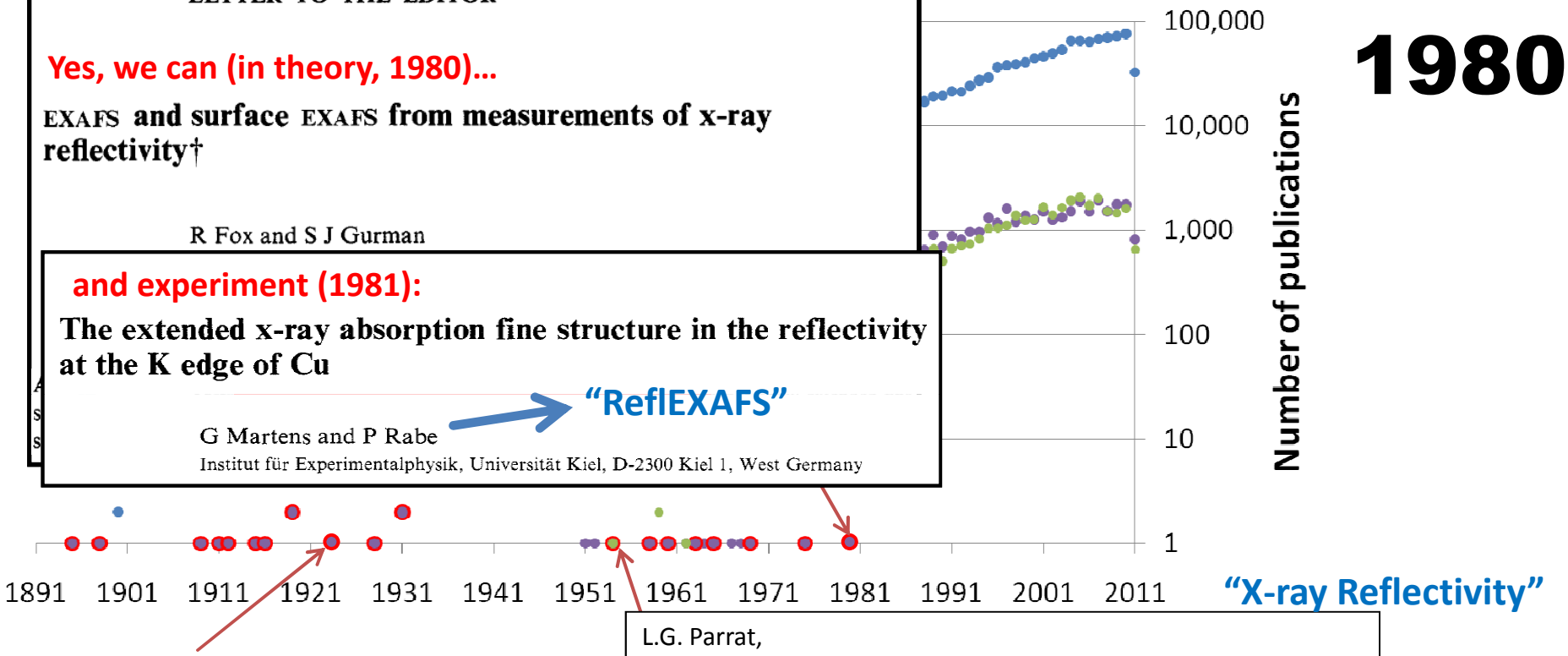

1980

"X-ray Reflectivity"

A.H. Compton,
The Total Reflection of X-rays,
Philosophical Magazine 45 (1923) 1121-1132.
reprinted in:
R.S. Shankland (Ed.), *Scientific Papers of Arthur Holly Compton: X-Ray and Other Studies*, University of Chicago Press, Chicago, 1973.

L.G. Parrat,
Surface Studies of Solids by Total Reflection of X-Rays
Physical Review, Vol 95, 2, 1954

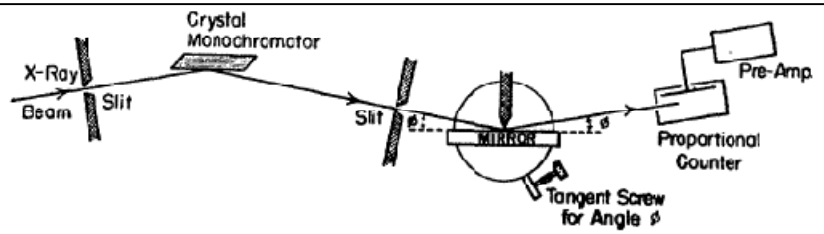

FIG. 1. Experimental arrangement for the x-ray total reflection method of studying smooth solid surfaces.

Total (external) reflection of X-rays

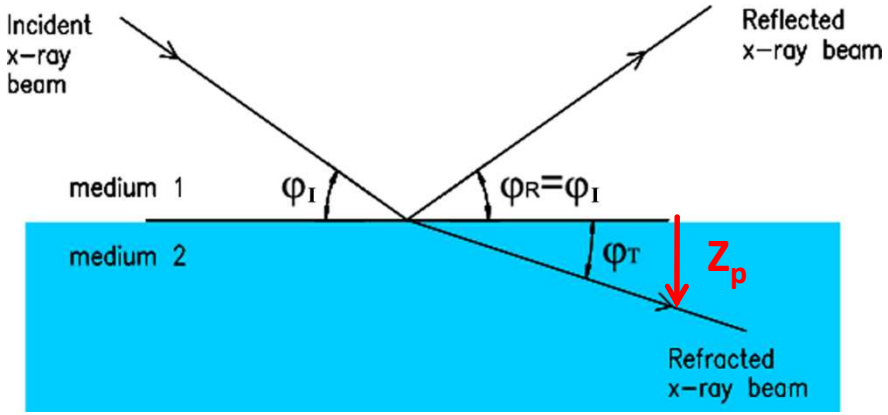

Sketch of optical paths of incident, reflected and transmitted beams at the interface of two media. The refraction index of medium 1 (usually vacuum or air) is larger that that of medium 2 (the reflector material).

Complex refraction index n:

n (x-ray range) = 1- δ - iβ

δ ~ 10^{-6} β ~ 10^{-8}

φ critical ≈ $\sqrt{2\delta}$

Absorption

Dispersion

φ critical
(Si, 17.5 keV) ≈ 0.1° ≈ 1.75 mrad
(Si, 500 eV) ≈ 3.7° ≈ 64.6 mrad

wavelength of the incident radiation

Atomic scattering factors

$$n = 1 - N_A \frac{r_0 \lambda^2}{2\pi} \frac{\rho}{A} (f_1 + i f_2)$$

'Absorption' term: $\beta = N_A \frac{r_0 \lambda^2}{2\pi} \frac{\rho}{A} f_2 = \frac{\lambda \rho}{4\pi} \tau$

photo-absorption coefficient

The penetration depth Z_P is defined as the distance measured normal to the samples surface where the intensity of the penetrating (here the refracted) beam is reduced by a factor of ***e***

$$Z_P = \frac{1}{\mu(E)} \varphi_T$$

$$\mu(E) = \tau(E) + \sigma_{coh}(E) + \sigma_{incoh}(E)$$

(sin $\varphi_T \approx \varphi_T$)

Snell's law: $\frac{n_{medium\,1}}{n_{medium\,2}} = \frac{\cos\varphi_T}{\cos\varphi_I}$

$I(x) = I_0 e^{-\mu(E)x}$ … Beer-Lambert's law

Total (external) reflection of X-rays

Penetration depth as a function of incident angle:
(calculated for Si substrate, 17.4 keV x-ray energy)

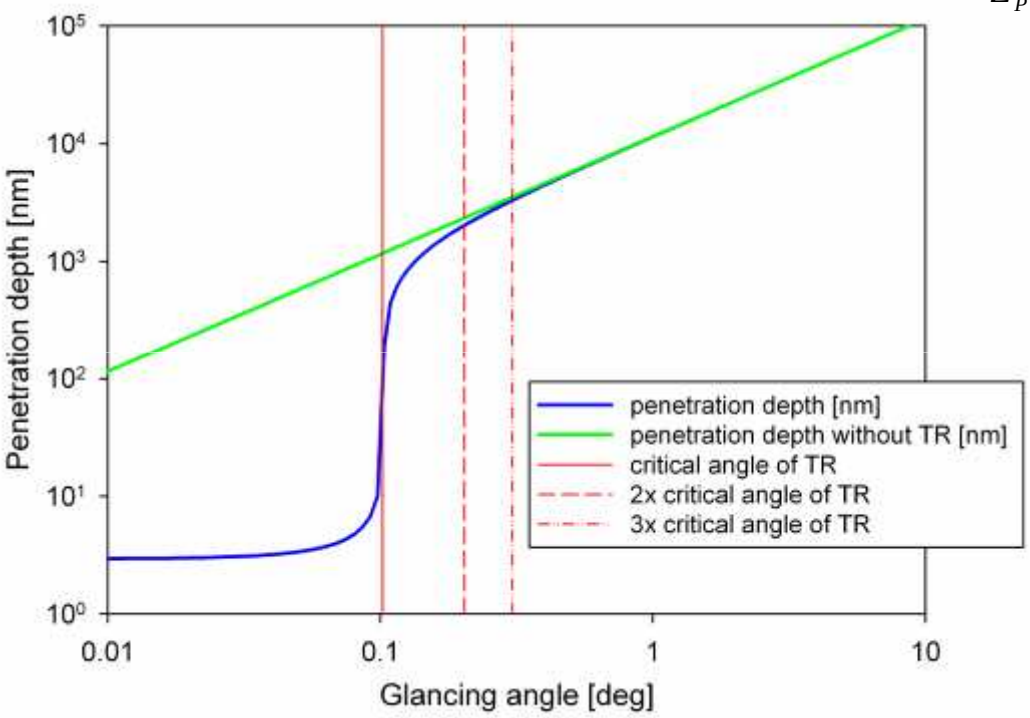

Idea to measure XAFS:

$$I_r + I_{absorb} = I_0 \quad \Leftrightarrow \quad 1 - \frac{I_r}{I_0} \propto \mu(E)$$

But: the penetration depth Z_P is also a function of energy, $z_P = f(\varphi_I, E)$, because f_1, f_2 are functions of energy

The penetration depth:

$$Z_P = \frac{1}{\mu(E)}\varphi_T \qquad \text{Snell's law: } \frac{n_{medium\,1}}{n_{medium\,2}} = \frac{\cos\varphi_T}{\cos\varphi_I}$$

[d'Acapito 03]

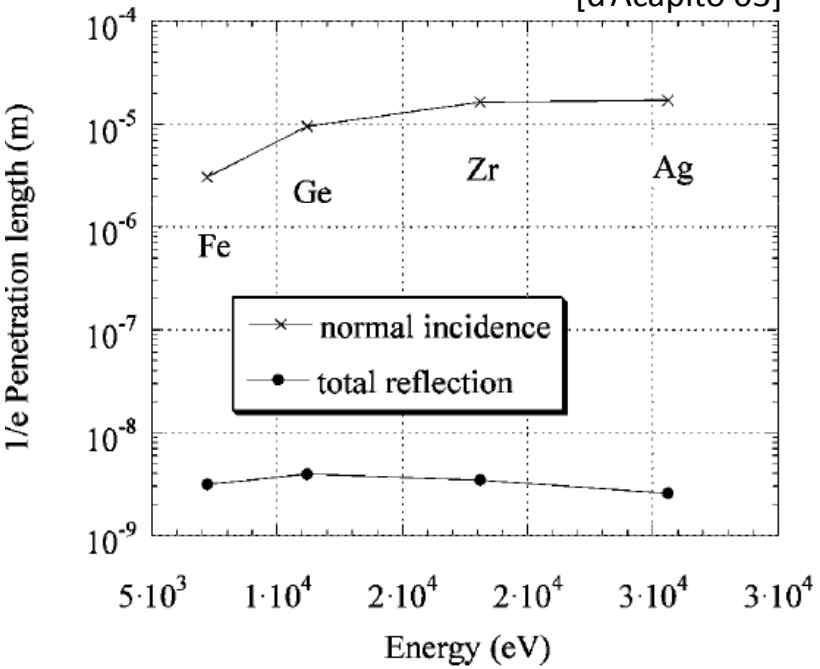

Figure 1
Comparison between the 1/e penetration lengths in a series of bulk elements in normal and total reflection conditions. The calculations were performed at an angle $\varphi = 0.8\varphi_c$ and at an energy 100 eV above the relative K absorption edges to simulate the beam penetration in a typical EXAFS energy range. Values are around tens of μm in the former case and a few nm in the latter case, with a drop of roughly four orders of magnitude when working in total reflection.

Total (external) reflection of X-rays

Penetration depth into substrate (e.g.Si) as a function of incident angle and energy

critical angle of TR

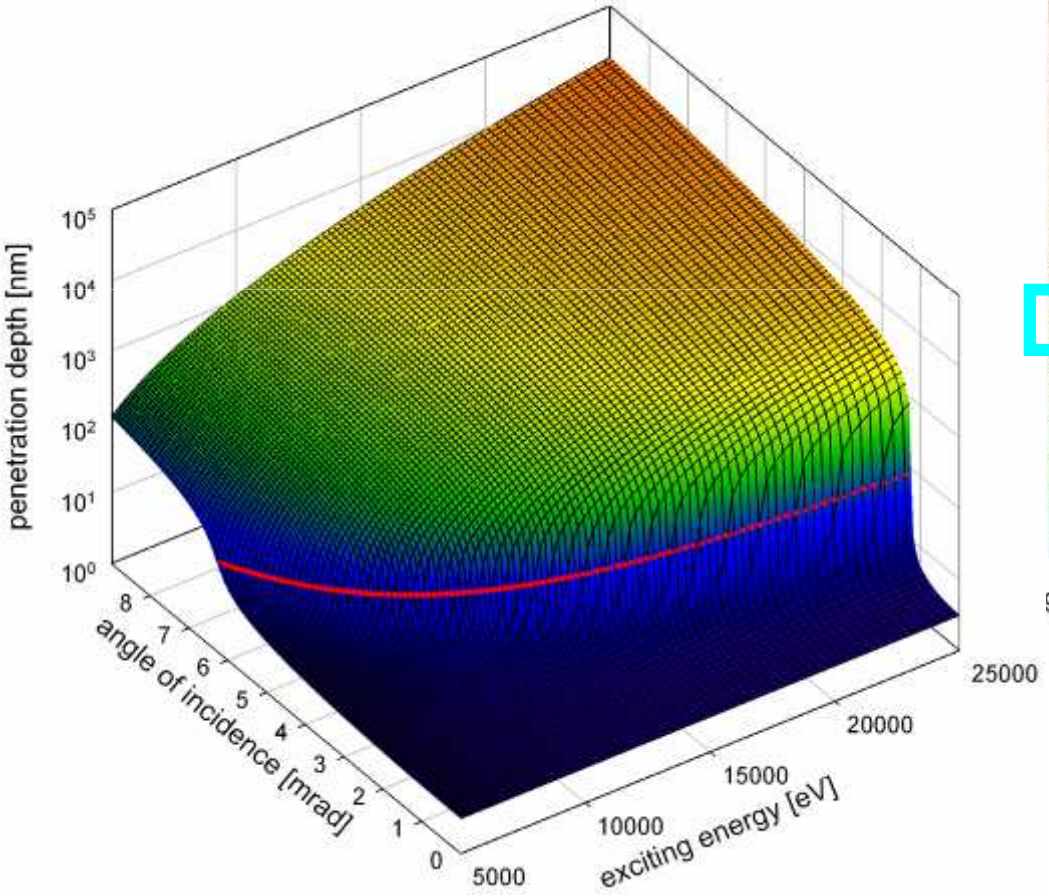

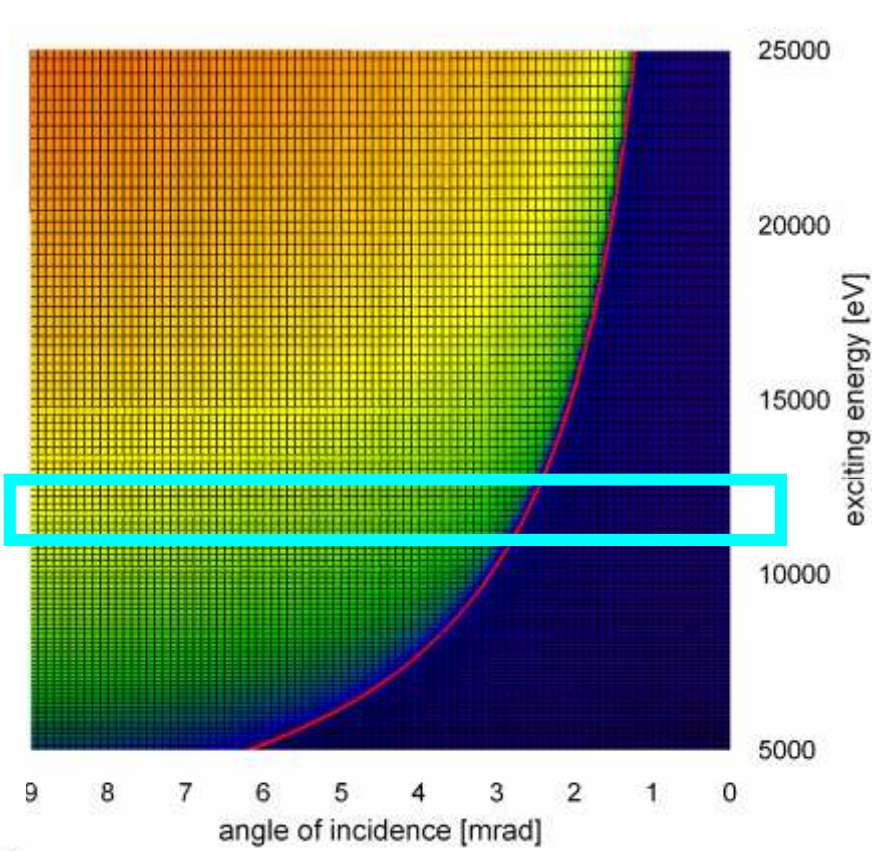

Exciting energy: 5 – 25keV
Angle of incidence: 0 – 9mrad
Penetration depth in log scale

Total (external) reflection of X-rays

Penetration depth into substrate (e.g. Si) as a function of incident angle and energy

Example: Arsenic EXAFS, typical range of energy (~1keV): 11800 – 12800 eV

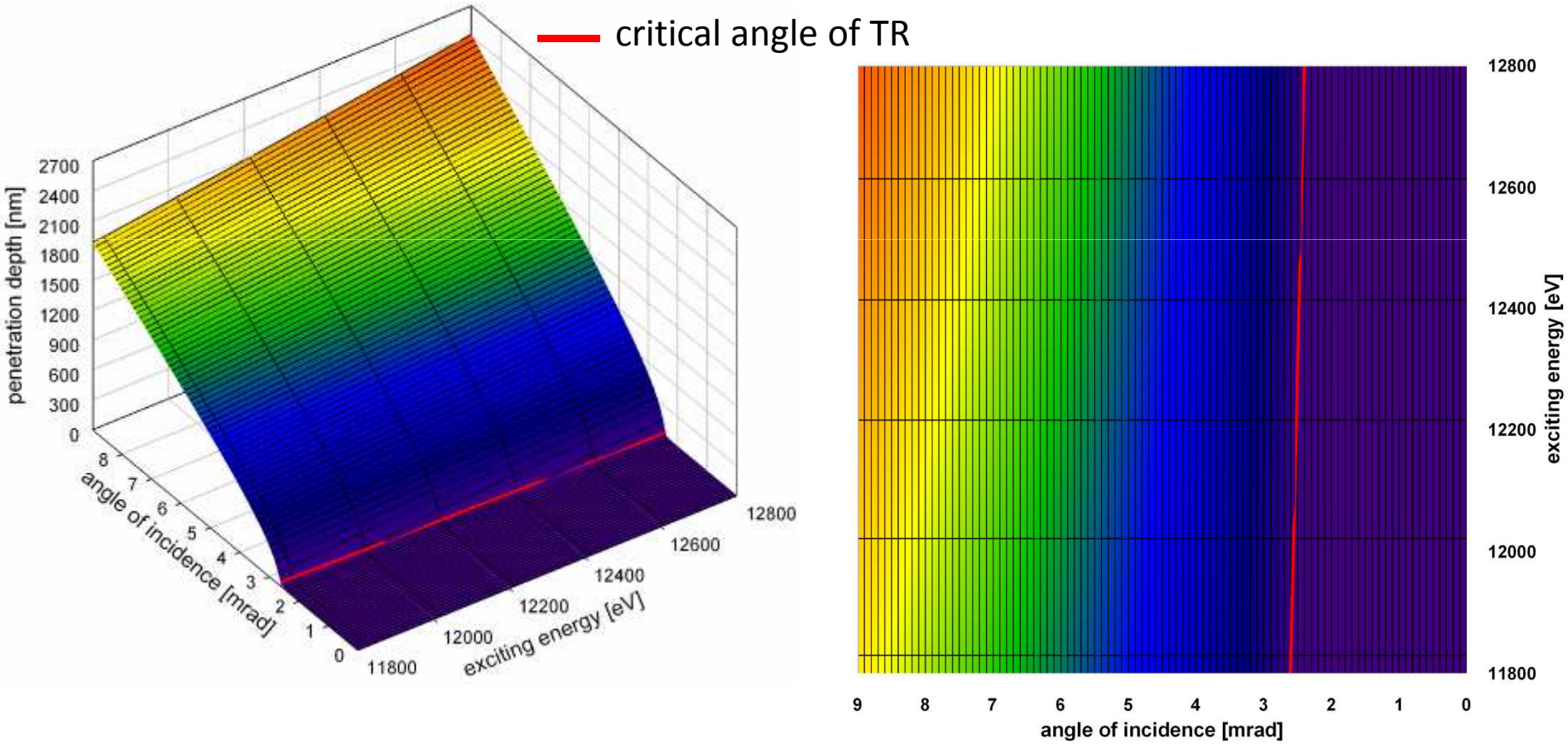

Total (external) reflection of X-rays

Penetration depth into substrate (e.g. Si) as a function of incident angle and energy

Anomalous dispersion:

Penetration depth = f (β, δ, angle of incidence, τ)
τ, β = f (f_2)
δ (Dispersion), critical angle of TR = f (f_1)
f_1, f_2 … atomic scattering factors

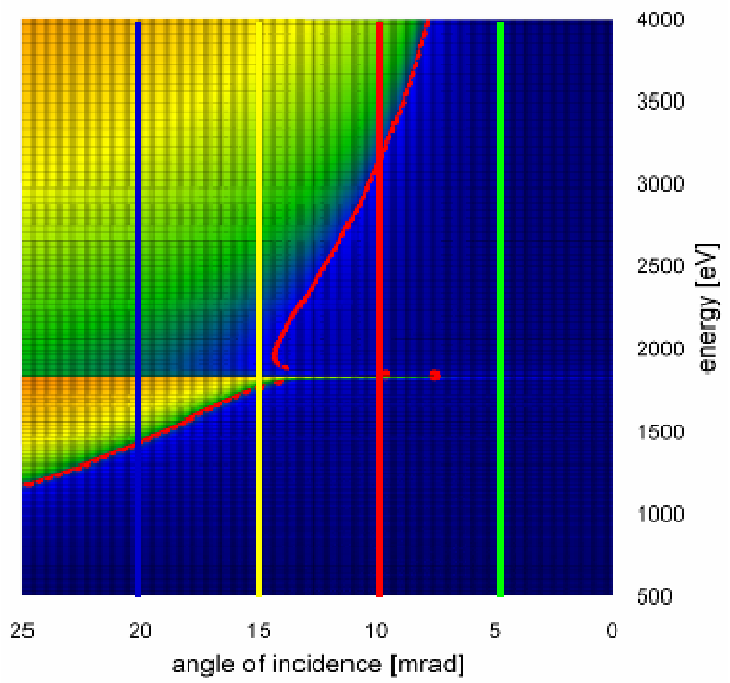

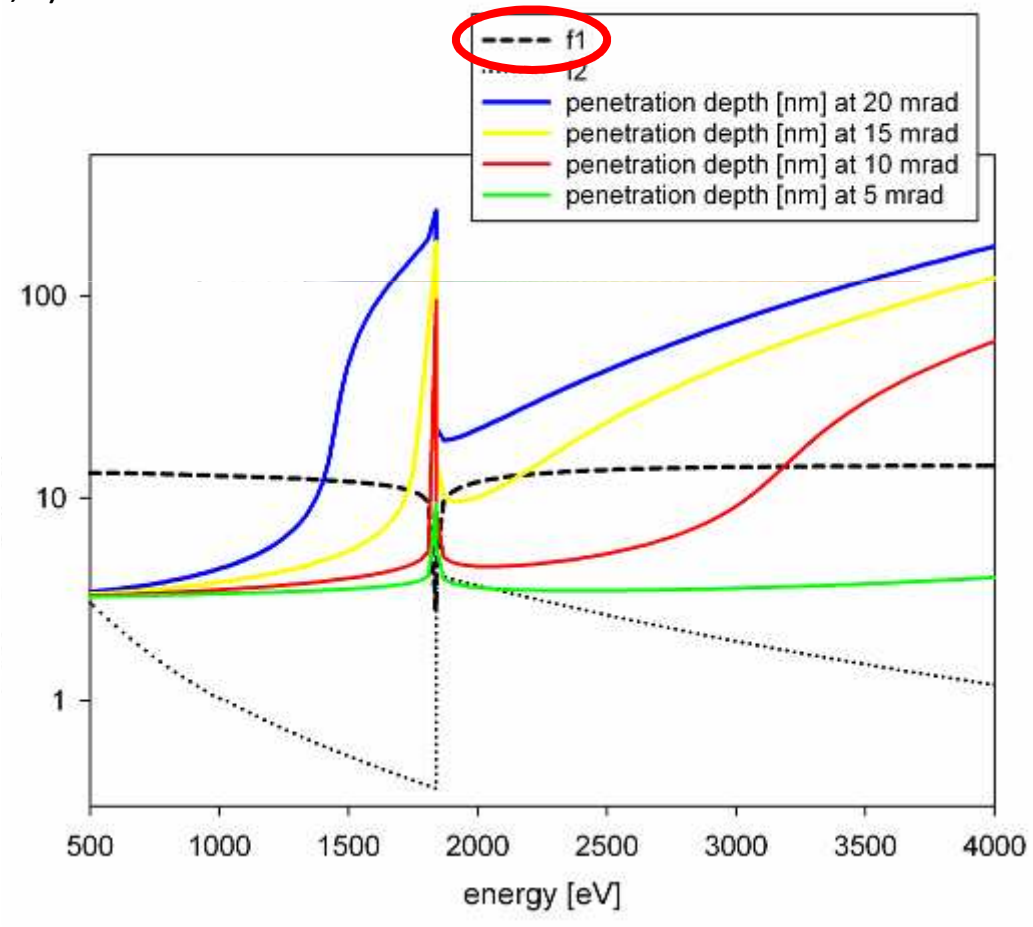

Total (external) reflection of X-rays

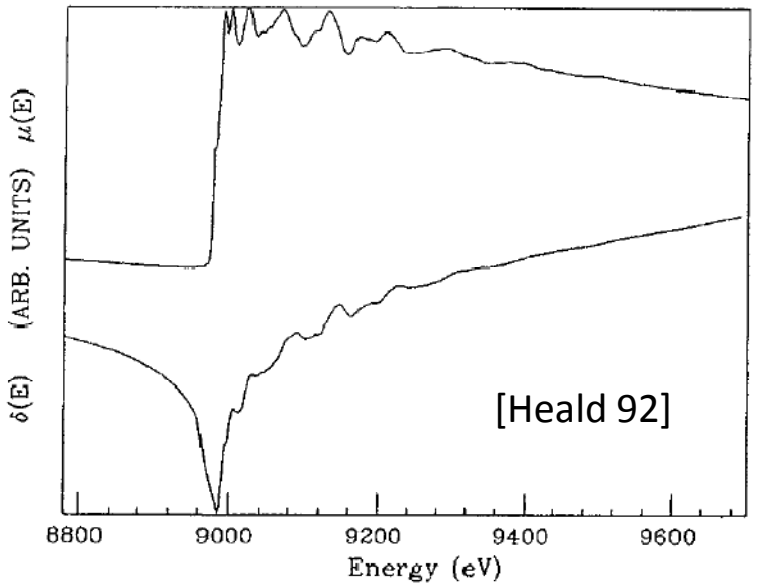

FIG. 1. Kramers-Kronig calculation of δ for Cu metal near the Cu K edge.

Anomalous dispersion:

Penetration depth = f (β, δ, angle of incidence, τ)
τ, β = f (f_2)
δ (Dispersion), φ_{crit}= f (f_1)
f_1, f_2 … atomic scattering factors

δ oscillations are 90° out of phase with normal EXAFS
=> distortion results in reduced amplitude & phase shift.

Challenges in ReflEXAFS/GI-EXAFS if element of interest forms the reflecting layer(s):

1) for $\varphi_I \approx \varphi_{crit}$ the edge is large, but strongly distorted by the anomalous dispersion effect
2) The absolute value of the reflectivity is unknown because of the roughness of the surface of the sample, together with the beam divergence which gives an overall slope to the reflectivity

Good news:

-) The distortions are small/negligible for ultra-thin layers (e.g. several atomic layers thickness) [Jiang 98]

Correction method(s) available:

-) Knowledge of δ, β over a long data range (Kramers-Kronig calculations) [Poumellec 89]
-) Derive an accurate model of the reflectivity from the sample. This can be done by fitting the angular dependence of the reflectivity to obtain the depth dependent density profile. [Heald 92]

SSRL

1984

J. A. del Cueto and N. J. Shevchik,
EXAFS of ultra thin layers of Cu
J. Phys. C: Solid State Phys., Vol. 11, 1978

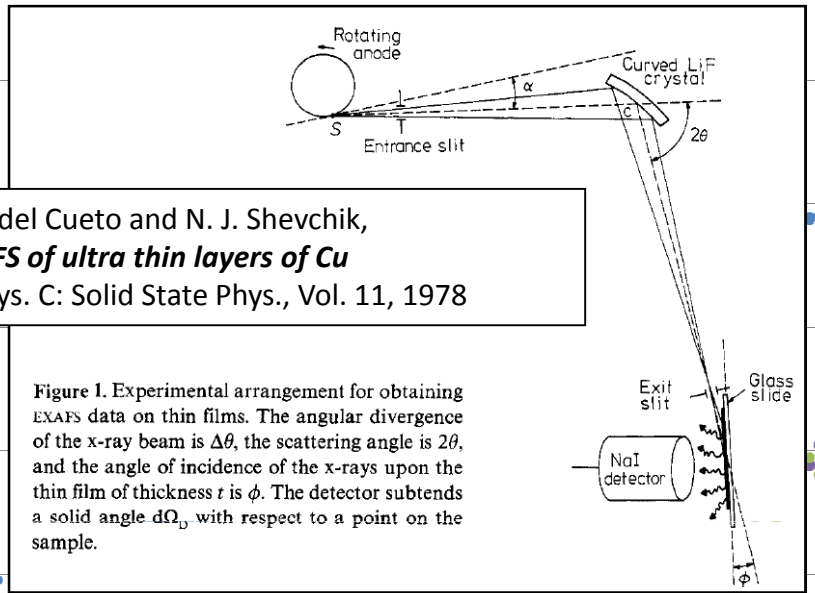

Figure 1. Experimental arrangement for obtaining EXAFS data on thin films. The angular divergence of the x-ray beam is $\Delta\theta$, the scattering angle is 2θ, and the angle of incidence of the x-rays upon the thin film of thickness t is ϕ. The detector subtends a solid angle $d\Omega_D$ with respect to a point on the sample.

L.G. Parrat,
Surface Studies of Solids by Total Reflection of X-Rays
Physical Review, Vol 95, 2, 1954

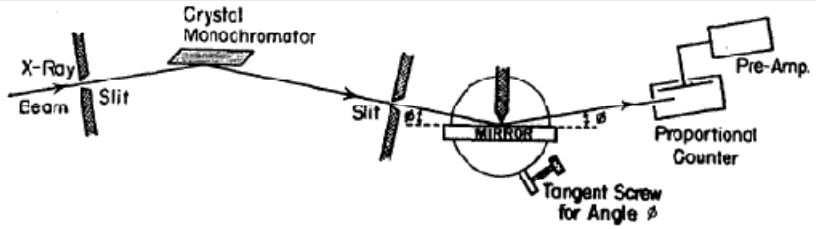

FIG. 1. Experimental arrangement for the x-ray total reflection method of studying smooth solid surfaces.

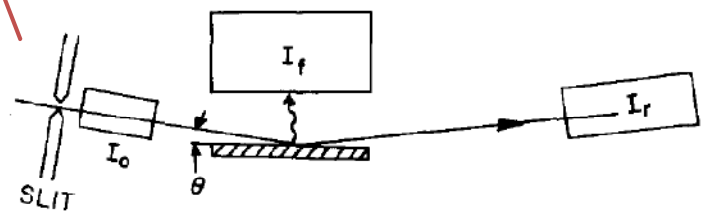

Fig. 1. Experimental arrangement. The three detectors are gas ionization detectors.

S.M. Heald, E. Keller, E.A. Stern,
Fluorescence Detection of Surface EXAFS
Physics Letters, 103A, 1984

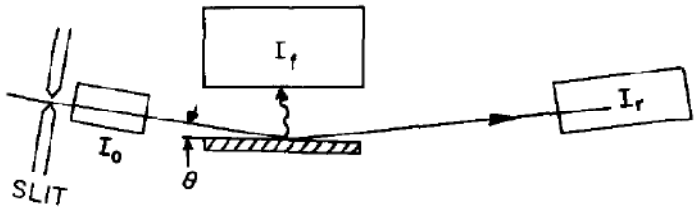

Fig. 1. Experimental arrangement. The three detectors are gas ionization detectors.

S.M. Heald, E. Keller, E.A. Stern,
Fluorescence Detection of Surface EXAFS
Physics Letters, 103A, 1984

- excellent S/N ratios
- wide applicability to surface and near surface systems
- detection of trace elements on surfaces

The possibilities for fluorescence detection of surface EXAFS are studied using thin films of gold on various substrates. For glancing incidence angles it is found that excellent signal to noise ratios can be obtained even for submonolayer films, demonstrating that the technique should have wide applicability to surface and near surface systems. In many cases the signal to noise is superior to electron detection techniques, and its sensitivity suggests the method may also be useful for detection of trace elements on surfaces.

Plus (for total reflection):
Interference of incident and reflected beam causes a standing wave field above the reflectors surface.

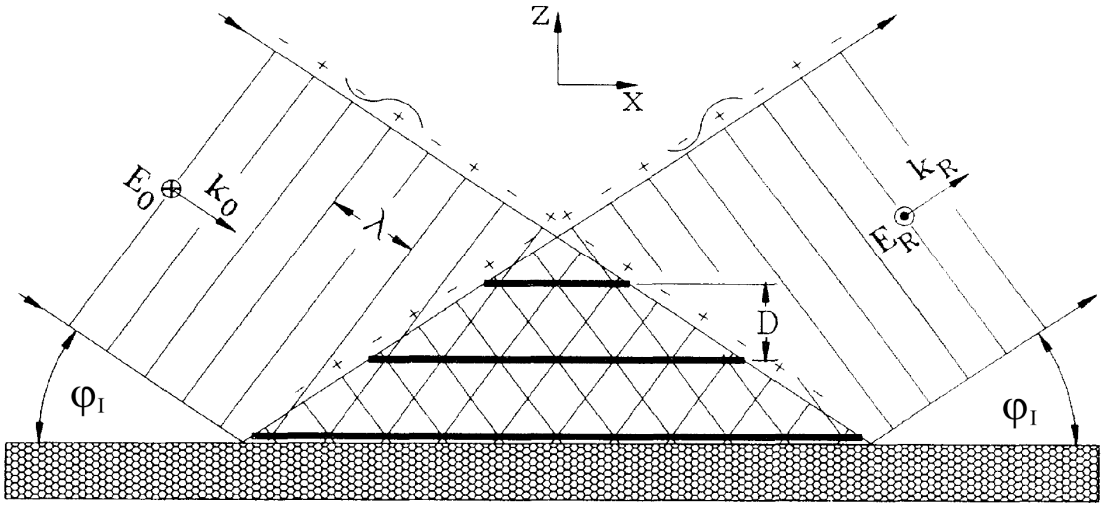

adapted from [Bedzyk 89]

Total (external) reflection of X-rays

n (x-ray range) = 1- δ - iβ

δ ~ 10^{-6} β ~ 10^{-8}

φ critical ≈ $\sqrt{2\delta}$

φ critical
(Si, 17.5 keV) ≈ 0.1° ≈ 1.75 mrad
(Si, 500 eV) ≈ 3.7° ≈ 64.6 mrad

The interference of incident and reflected beam causes a standing wave field above the reflectors surface.

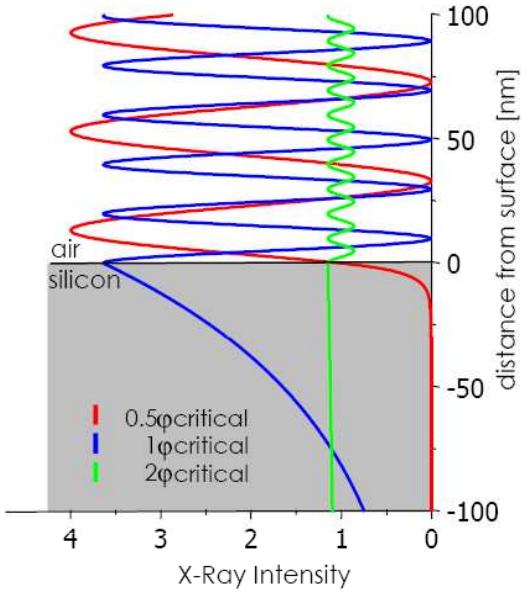

Characteristic shapes due the angular dependence of the fluorescence radiation for three different cases of atomic locations:

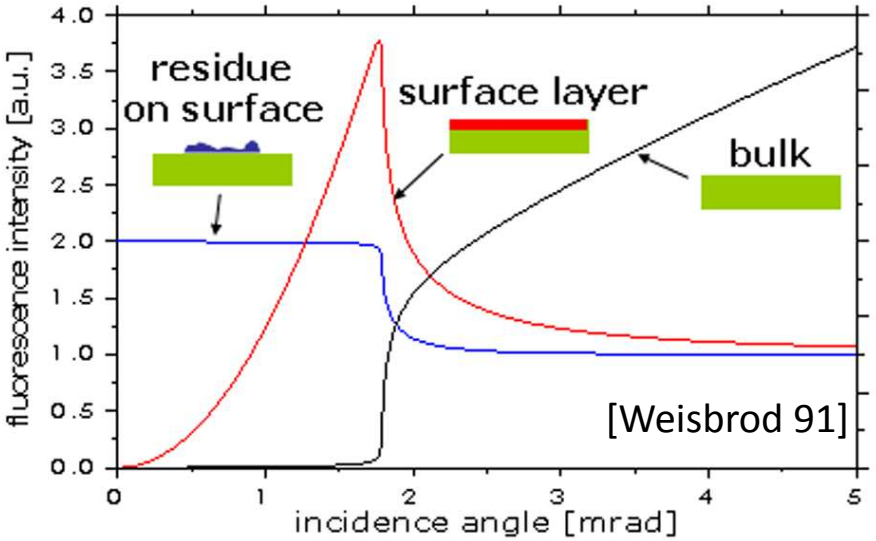

Intensity distribution in substrate as a function of incident angle and depth:

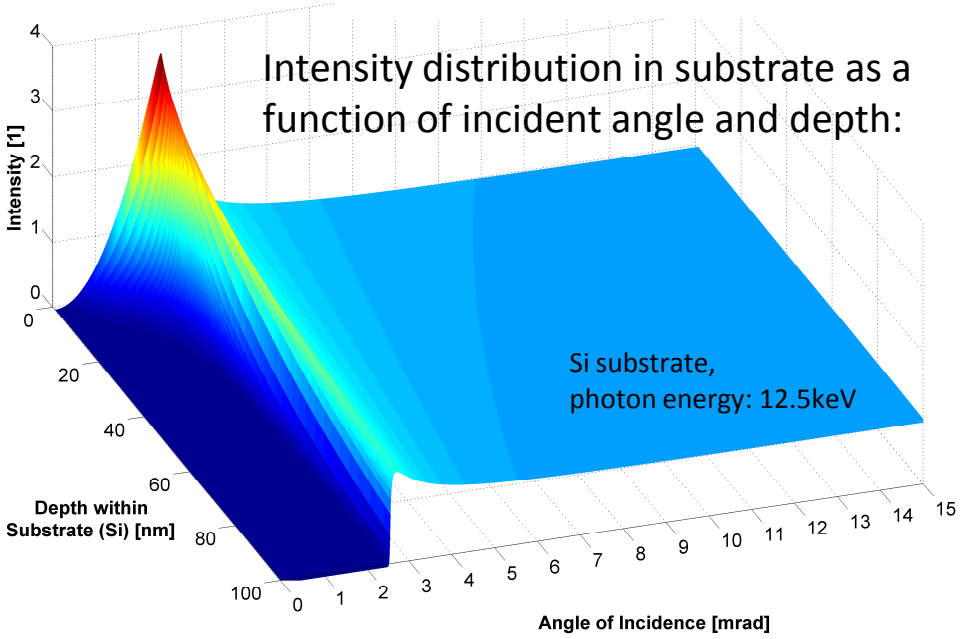

The x-ray standing wave (XSW) field

Challenge:
Influence of a finite coherence of the incident X-rays:
=> the number of nodes and antinodes in the intersection volume of the incident and reflected beam becomes limited.

But:
the high flux and natural collimation of a SR source allows small slits (typically <100 µm) and monochromators with high spectral resolution ($\Delta\lambda/\lambda \approx 10^{-4}$), dramatically reducing spatial and energy divergence, which, in turn, increases the longitudinal and transversal coherence lengths

[Krämer 07]

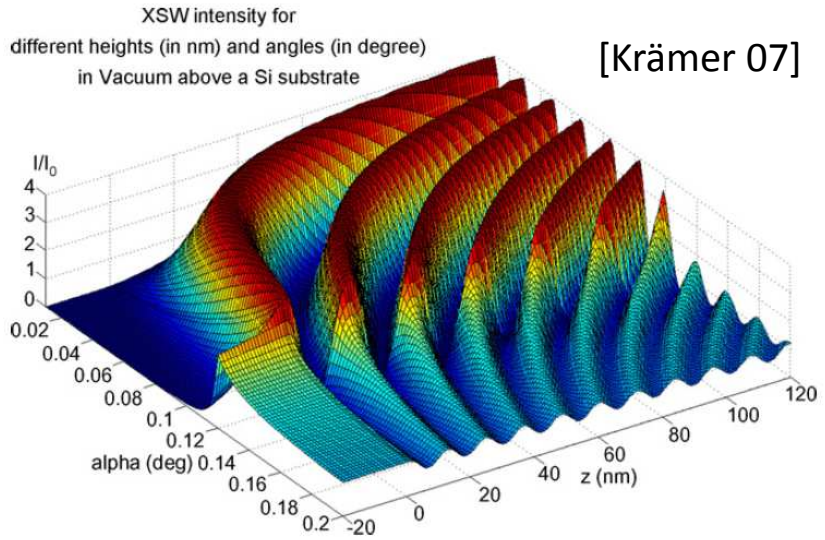

Fig. 5. 3D simulation of XSW in vacuum for a photon energy of 15 keV above a Si substrate for angles of incidence from 0.01° to 0.2° (left axis) and positions from 20 nm below to 120 nm above the surface (right axis). Intensity below the surface is decreasing exponentially with depth, above the surface oscillations occur with a maximum intensity of $4I_0$.

[Meirer 10]

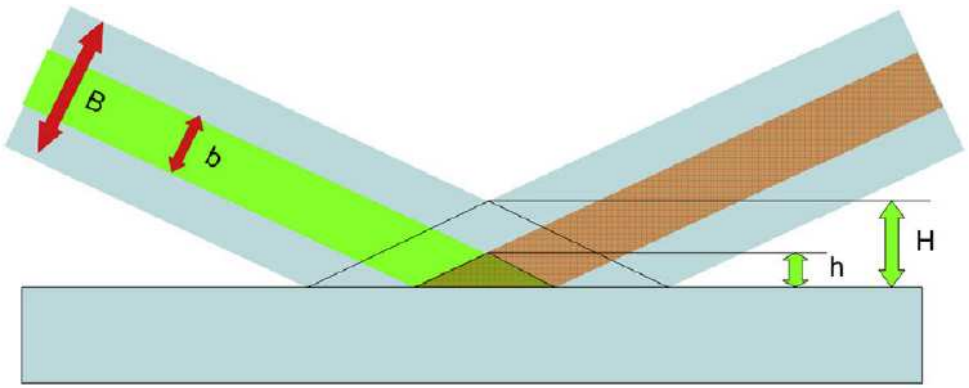

Figure 5. As Fig. 3 but considering the finite transverse coherence length of the X-ray beam causing b < B. Only a small volume close above the reflector surface contains interference fringes, the major part is filled by non-modulated double intensity of the non-interfering exciting and totally reflected X-rays (=> h < H).

Advantages of GI geometry

- background reduction in fluorescence spectra
- small distance sample ⇔ detector (~1mm) ⇨ large solid angle

} High sensitivity

- angle dependence of fluorescence signal ⇨ depth dependent information

Fluorescence spectra

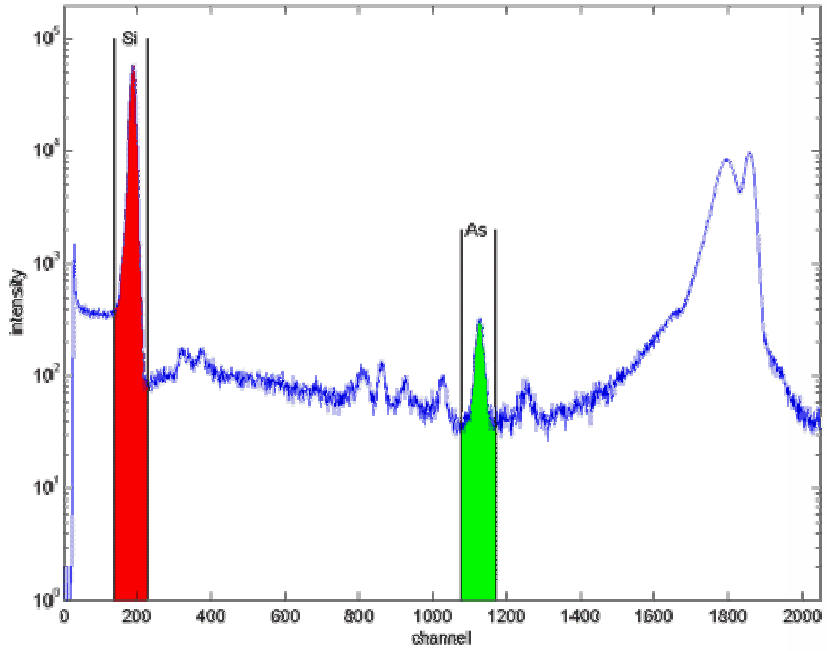

Angle profile

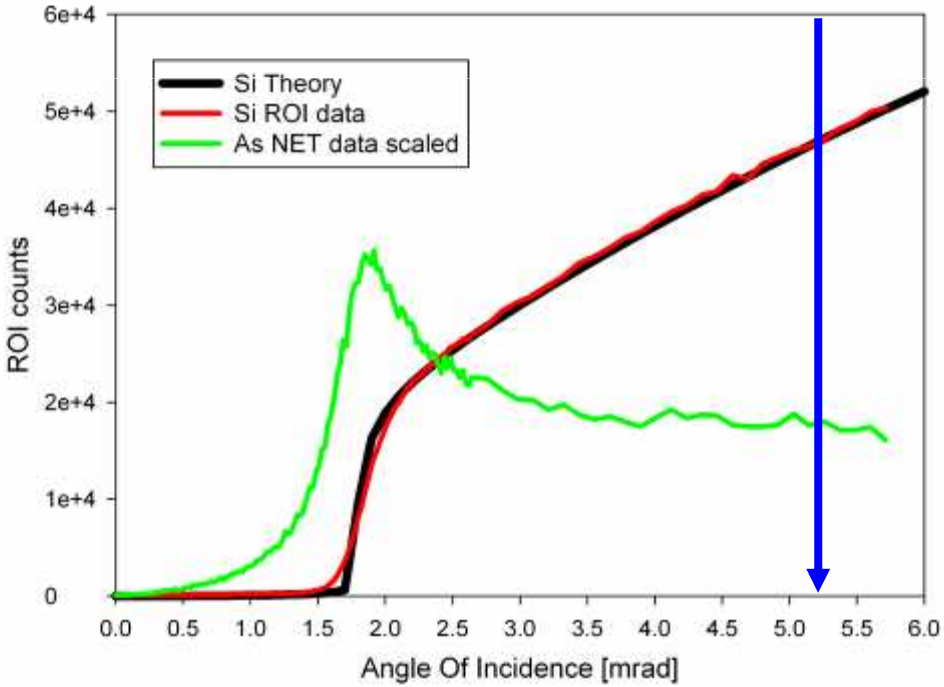

The self absorption effect in TXRF XAS

Sample (droplet) size becomes thickness, i.e. path that the primary beam crosses

⇨ Large or highly concentrated samples: penetration depth of incident beam < sample size

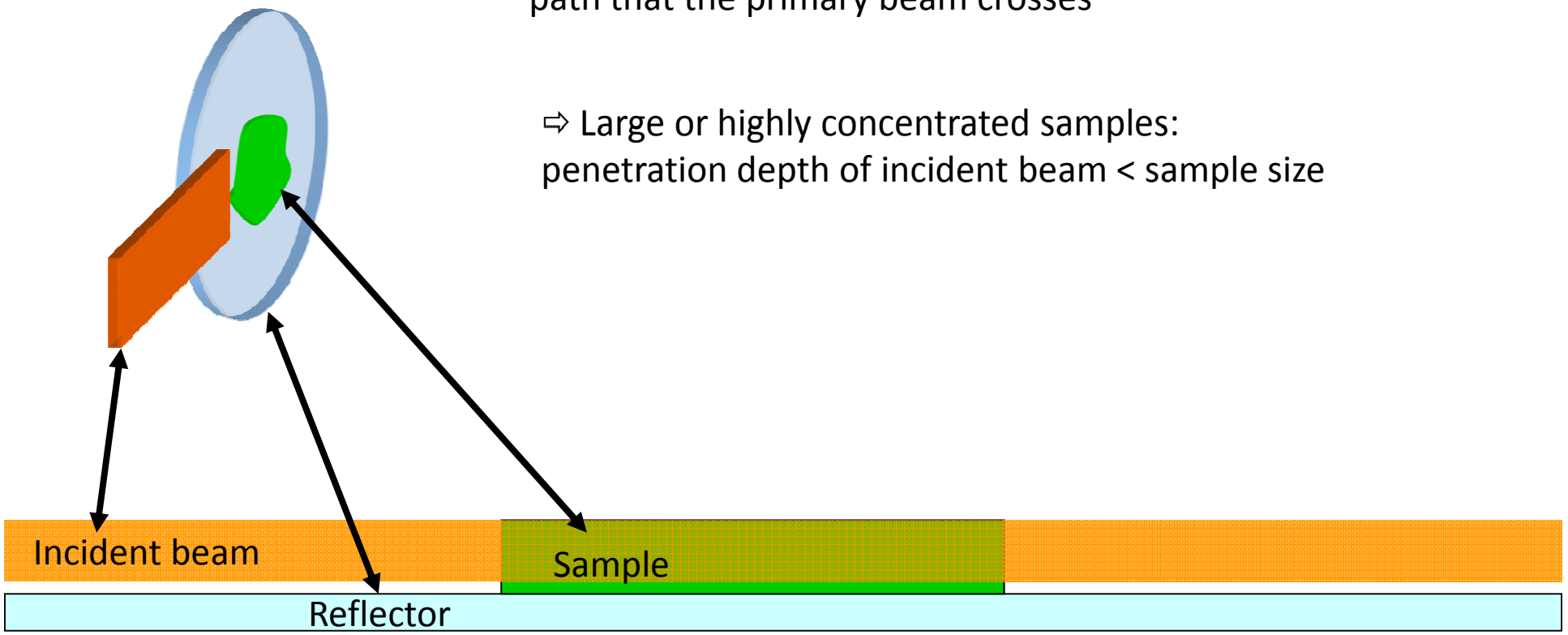

The self absorption effect in TXRF XAS

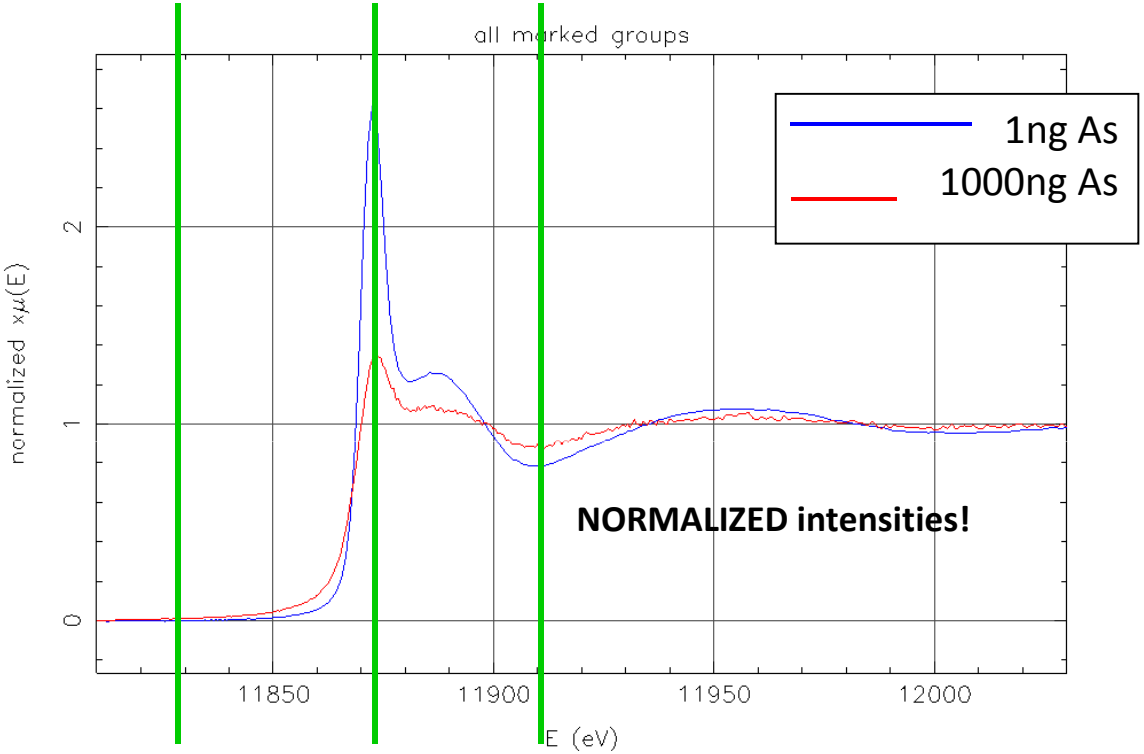

⇨ Large or concentrated samples: penetration depth < sample size

⇨ an increased absorption coefficient of an XAFS oscillation will decrease the penetration depth (and vice versa) and therefore the illuminated volume

⇨ the XAFS oscillations are attenuated or may disappear

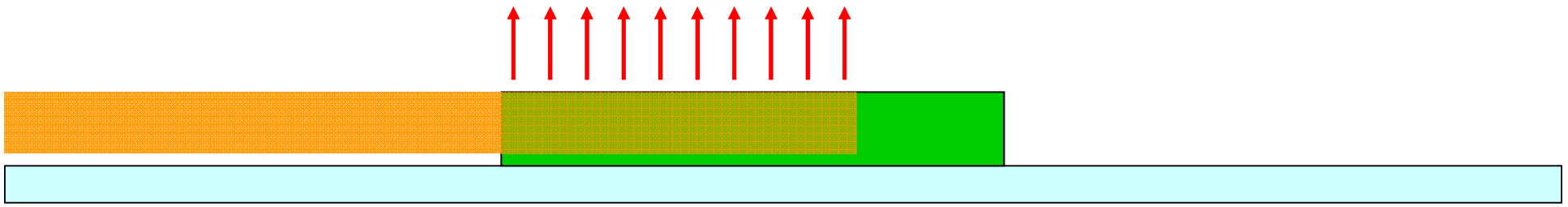

The self absorption effect in TXRF XAS

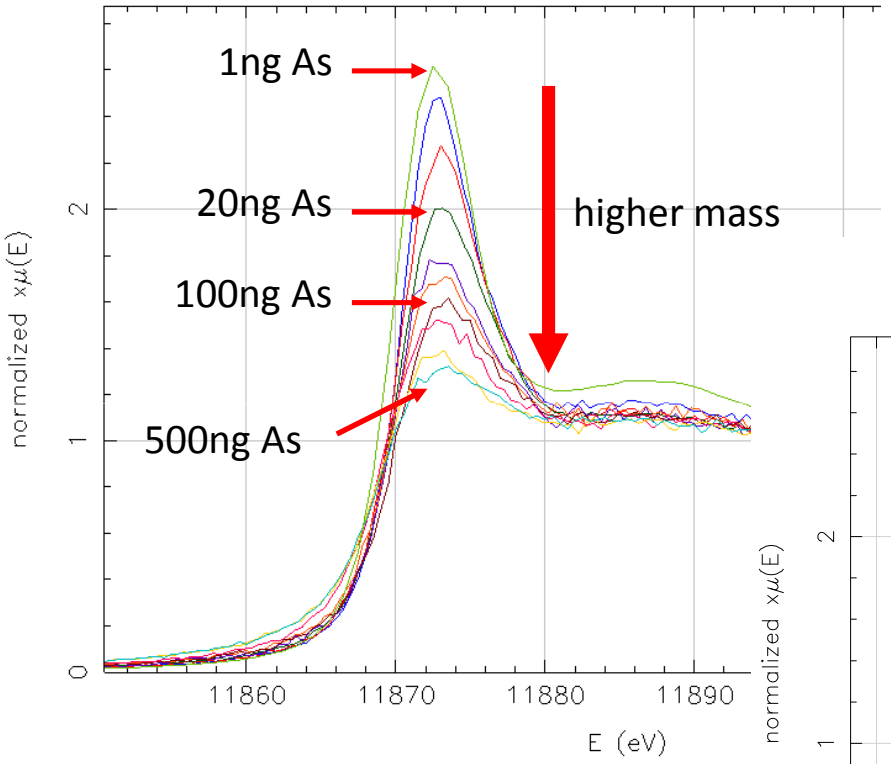

Series of different total amounts of Arsenic on sample carriers

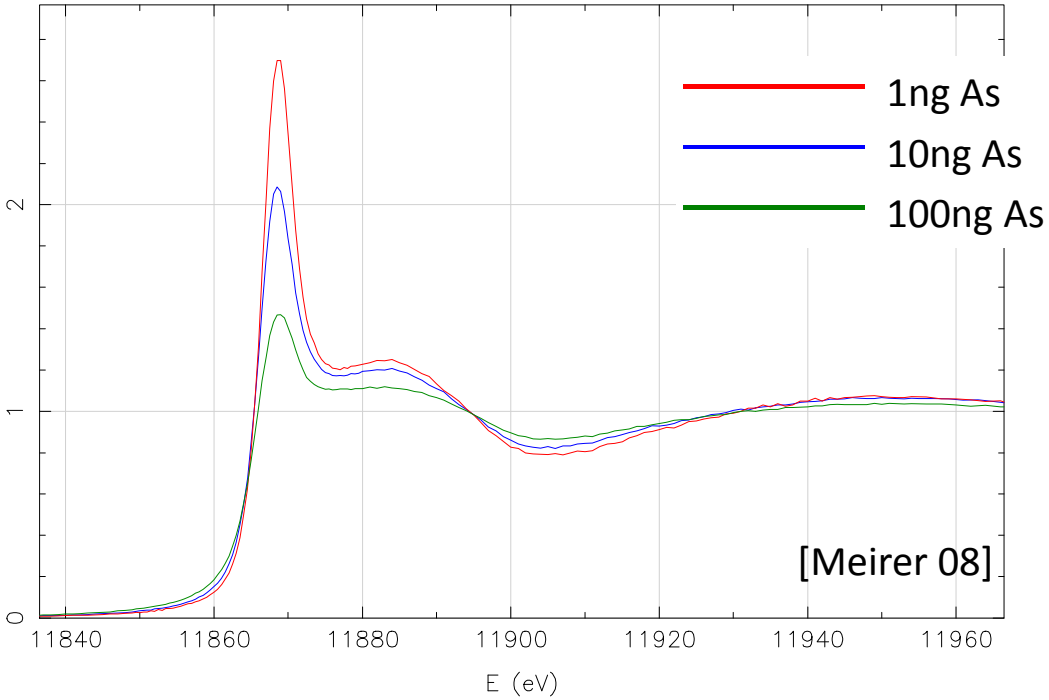

Damping of the XANES oscillations can be correlated to the mass of Arsenic

The self absorption effect – comparison of GI and GE setup

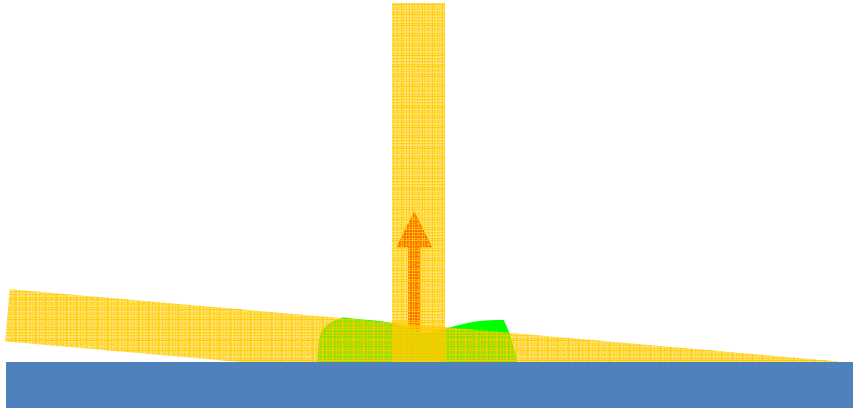

Minimized path length of the incident beam through the sample

⇒ Normal incidence-grazing-exit geometry (GE-setup) should not suffer from self-absorption effects in XAFS analysis but delivers equivalent information (optical reciprocity theorem [Becker 83])

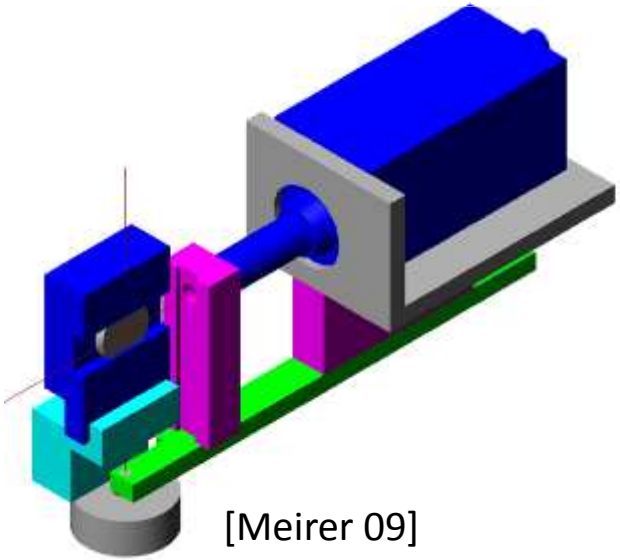

[Meirer 09]

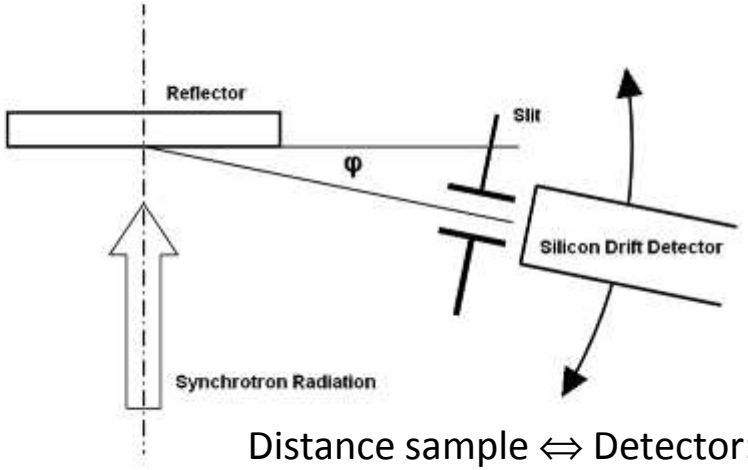

- Lightweight SDDs allow rotating the whole detector-slit system
- Center of rotation on reflector surface

Distance sample ⇔ Detector: 40mm
Slit-width: 40µm

The self absorption effect – comparison of GI and GE setup

- GE setup suffers minimally from self-absorption effects
- Shows lower sensitivity than GI-setup

$\Rightarrow$ difficult to apply to XAFS analysis of trace amounts (few nanograms) of samples

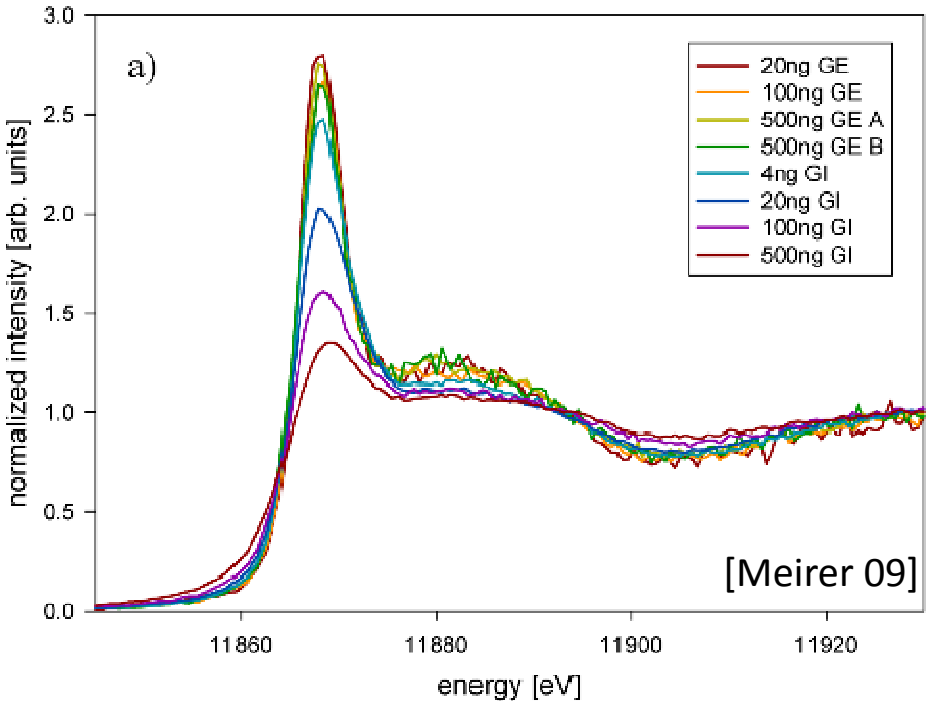

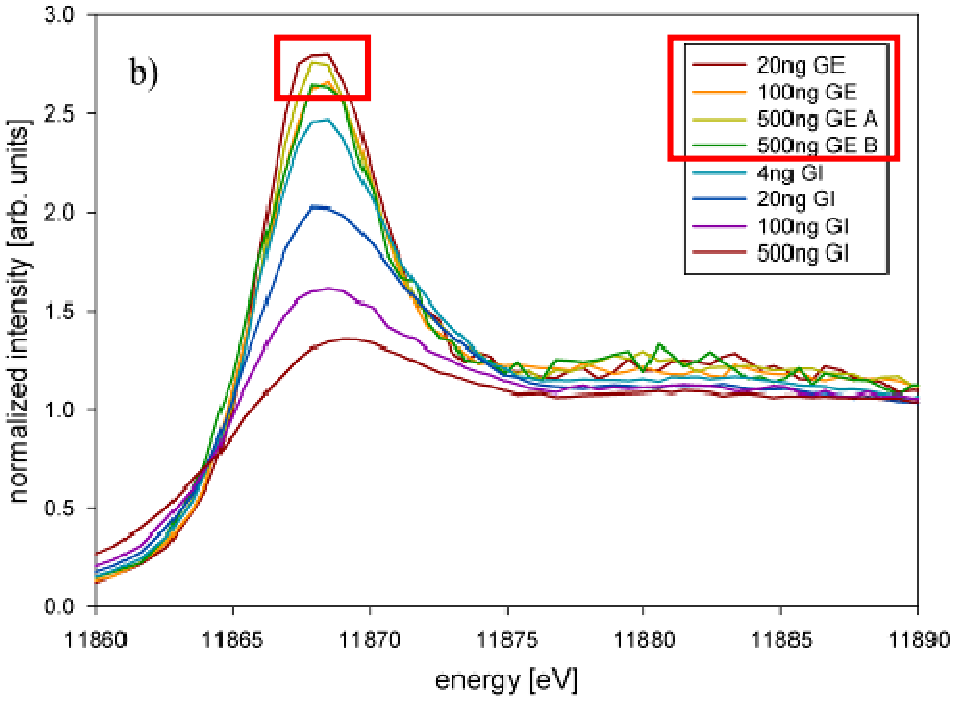

References:

[Stöhr 96]	J. Stöhr, *NEXAFS Spectroscopy*, ed. G. Ertl, et al. 1996, Berlin, Heidelberg, New York: Springer-Verlag.
[Lagarde 01]	P. Lagarde, Ultramicroscopy 86 (2001) 255–263
[d'Acapito 03]	J. Synchrotron Rad. (2003). 10, 260-264
[Heald 92]	S. M. Heald, Rev. Sci. Instrum. 63 (1), 1992
[Poumellec 89]	B. Poumellec, R. Cortes, F. Lagnel, and G. Tourillon. Physica B, 158, 282 (1989).
[Jiang 98]	D.T. Jiang and E.D. Crozier, Can. J. Phys 76: 621–643 (1998)
[Weisbrod 91]	U. Weisbrod, R. Gutschke, J. Knoth, H. Schwenke, Fresenius' Journal of Analytical Chemistry 341 (1991) 83-86
[Bedzyk 89]	M.J. Bedzyk, G.M. Bommarito, J.S. Schildkraut, Physical Review Letters 62 (1989) 1376
[Meirer 10]	F. Meirer, A. Singh, G. Pepponi, C. Streli, T. Homma, P. Pianetta, Trends in Analytical Chemistry, Vol. 29, No. 6, 2010
[Krämer 07]	M. Krämer, A. von Bohlen, C. Sternemann, M. Paulus, R. Hergenröder, Applied Surface Science 253 (2007) 3533–3542
[Meirer 08]	F. Meirer, G. Pepponi, C. Streli, P. Wobrauschek, P. Kregsamer, N. Zoeger, G. Falkenberg, Spectrochimica Acta Part B 63 (2008) 1496–1502
[Becker 83]	R. S. Becker, J. A. Golovchenko, J. R. Patel, Phys. Rev. Lett. 50, 153 (1983).
[Meirer 09]	F. Meirer, G. Pepponi, C. Streli, P. Wobrauschek, N. Zoeger, J. Appl. Phys. 105, 074906 (2009)